RNA (2001), *7*:553–564. Cambridge University Press. Printed in the USA.

Distinct modes of mature and precursor tRNA binding to *Escherichia coli* RNase P RNA revealed by NAIM analyses

CORINNA HEIDE,[1] SILKE BUSCH,[1,2] RALPH FELTENS,[1] and ROLAND K. HARTMANN[1]

[1]Medizinische Universität zu Lübeck, Institut für Biochemie, D-23538 Lübeck, Germany

ABSTRACT

We have analyzed by nucleotide analog interference mapping (NAIM) pools of precursor or mature tRNA molecules, carrying a low level of R_p-RMPαS (R = A, G, I) or R_p-c7-deaza-RMPαS (R = A, G) modifications, to identify functional groups that contribute to the specific interaction with and processing efficiency by *Escherichia coli* RNase P RNA. The majority of interferences were found in the acceptor stem, T arm, and D arm, including the strongest effects observed at positions G19, G53, A58, and G71. In some cases (interferences at G5, G18, and G71), the affected functional groups are candidates for direct contacts with RNase P RNA. Several modifications disrupt intramolecular tertiary contacts known to stabilize the authentic tRNA fold. Such indirect interference effects were informative as well, because they allowed us to compare the structural constraints required for ptRNA processing versus product binding. Our ptRNA processing and mature tRNA binding NAIM analyses revealed overlapping but nonidentical patterns of interference effects, suggesting that substrate binding and cleavage involves binding modes or conformational states distinct from the binding mode of mature tRNA, the product of the reaction.

Keywords: c7-deaza-modifications; inosine modifications; nucleotide analog interference mapping (NAIM); ptRNA processing by *E. coli* RNase P RNA; tRNA binding to *E. coli* RNase P RNA

INTRODUCTION

Ribonuclease P (RNase P) is an essential endoribonuclease that generates the mature 5′ ends of tRNAs. The RNA subunits of bacterial and some archaeal RNase P enzymes are catalytically active in vitro in the absence of their protein component(s) at elevated salt concentrations (Guerrier-Takada et al., 1983; Pannucci et al., 1999). Bacterial RNase P RNAs mainly recognize the acceptor stem and T arm modules of tRNA molecules (reviewed in Frank & Pace, 1998). In addition, the NCCA 3′ terminus of tRNAs makes crucial contacts with the J15/16 region of *Escherichia coli* RNase P RNA (reviewed in Frank & Pace, 1998, and Altman & Kirsebom, 1999). This interaction provides a substantial contribution to the free energy of precursor and mature tRNA binding (Kirsebom & Svärd, 1994; Oh & Pace, 1994; Hardt et al., 1995a; Oh et al., 1998; Busch et al., 2000).

Reprint requests to: Roland K. Hartmann, Medizinische Universität zu Lübeck, Institut für Biochemie, Ratzeburger Allee 160, D-23538 Lübeck, Germany; e-mail: hartmann@biochem.mu-luebeck.de.

[2]Present address: Universitätsklinikum Tübingen, Institut für Pathologie, Abteilung Molekulare Pathologie, Liebermeisterstr. 8, 72076 Tübingen, Germany.

Krupp and coworkers identified positions in precursor tRNAs (ptRNAs), where R_p-phosphorothioates, 2′-deoxy modifications, purine N7 alkylation, and oximido modifications at C4 of uridines interfered with processing by *E. coli* RNase P RNA (Kahle et al., 1990b; Gaur & Krupp, 1993; Conrad et al., 1995). Interference effects were observed in the acceptor stem and T arm, identifying functional groups in tRNA that are candidates for direct contact to the ribozyme. More recently, Pan and coworkers reported that the 2′-hydroxyl groups of $tRNA^{Phe}$ residues 54, 56, 61, and 62 directly participate in ptRNA binding to *Bacillus subtilis* RNase P RNA (Loria & Pan, 1997). Results from crosslinking studies have been interpreted to indicate that precursor and mature tRNA do not bind to the surface of *E. coli* RNase P RNA in precisely identical fashion (Westhof et al., 1996), and further suggested more than one substrate binding mode (Kufel & Kirsebom, 1996; Pomeranz Krummel & Altman, 1999). In some cases, the 5′ leader sequence may determine the mode of substrate binding (Guerrier-Takada & Altman, 1993). Nucleotide analog interference mapping (NAIM) and phosphorothioate footprinting experiments (Gaur & Krupp, 1993; Conrad et al., 1995; Gaur et al., 1996) have provided evidence that tRNAs with short and

long extra arms interact differently with *E. coli* RNase P RNA.

Here we have utilized, for the first time, c7-deaza and inosine modifications to study the role of N7 positions of purines as well as 2-NH_2 groups of guanosines in a tRNA for efficient processing by and binding to *E. coli* RNase P RNA. Precursor $tRNA^{Gly}$ processing and mature $tRNA^{Gly}$ binding NAIM analyses revealed overlapping but nonidentical interference patterns. Our results indicate distinct binding modes for precursor and mature $tRNA^{Gly}$.

RESULTS

Phosphorothioate, c7-deaza, and inosine modifications in $ptRNA^{Gly}$ that interfered with processing by RNase P RNA

For the transcription of partially modified pools of $ptRNA^{Gly}$, about 10% of ATP or GTP was replaced with the corresponding analog (Fig. 1). The intensity of iodine hydrolysis bands was the same, by visual inspection, for transcripts carrying only the phosphorothioate (termed thioate in the following) modification and those carrying a thioate/purine double modification. Because S_p-NTPαS analogs are known to be incorporated by T7 RNA polymerase with roughly the same efficiency as regular nucleotides (Christian & Yarus, 1992), it is likely that all transcripts had about 10% of their A or G residues replaced with the analog.

Processing interference experiments were initially performed under single turnover conditions with trace amounts (<1 nM) of partially modified 3′-^{32}P-labeled $ptRNA^{Gly}$ pools in the presence of 0.1 μM *E. coli* RNase P RNA in 50 mM MES, pH 6.0 (at 37 °C), 1 M NH_4OAc, and 15 mM Mg^{2+}. Under these conditions, the ribozyme concentration is not saturating (single turnover $K_m = 0.15$ μM; Warnecke et al., 1996). Processing reactions were stopped when 30–50% of the substrate had been converted to product, followed by separation of ptRNAs and mature tRNA products on denaturing gels and analysis of both RNA fractions by iodine hydrolysis (see Materials and Methods). Interference effects were classified as weak (<25%), moderate (25–50%), and strong (>50%). Interference effects with average values <10% were considered insignificant. Thioate-specific interference effects were observed at G24, G40, G49, A57, and G71 (Figs. 2 and 3A). Thioate interference at G71 was enhanced in the presence of an additional c7-deaza or inosine modification, thus showing the importance of the phosphate and N7 and 2-NH_2 functional groups at this position (Fig. 3A). Sites of c7-deaza interference further included A14, G53, and A58, and inosine interference was seen at G5, G19, G28, G39, G52, and G53. (Figs. 2 and 3A). The two strongest interferences were observed at A58 (c7-deaza) and G53 (inosine).

We further analyzed the effect of modifications at G + 1. This was accomplished by comparing the radioactivity in bands resulting from iodine hydrolysis 5′ of G + 1 in the original ptRNA pool and in the unreacted ptRNA fraction remaining after about 30–50% substrate conversion. With an R_p-phosphorothioate modification 5′ of G + 1, the corresponding iodine hydrolysis signal was enhanced by an average factor of 1.5 in the unreacted ptRNA fraction in comparison with the original ptRNA pool (data not shown). This is consistent with the finding that an R_p-phosphorothioate modification 5′ of G + 1 strongly inhibits processing in the presence of Mg^{2+} (Warnecke et al., 1996). An additional c7-deaza or inosine modification did not enhance interference at G + 1 to a statistically meaningful extent, indicating that the thioate modification at this position dominated the interference effect.

Because buffer conditions and RNA concentrations were different in the ptRNA processing (Figs. 2 and 3A) and the tRNA binding assay (Figs. 3B and 4; see below), we were concerned that observed differences in the interference pattern might have been primarily due to the different assay conditions, that is, the lower pH (6.0 versus 7.0) and Mg^{2+} concentration (15 versus 100 mM) in the processing assay. We therefore performed the cleavage interference assay at the same pH, salt, and RNA concentrations as used for the tRNA binding assay.

Under "tRNA binding conditions," cleavage interference effects were attenuated or became insignificant (Fig. 3A, values in parentheses; Fig. 5A versus 5B). However, no new sites of interference were observed, and the c7-deaza effect at A58 remained substantial

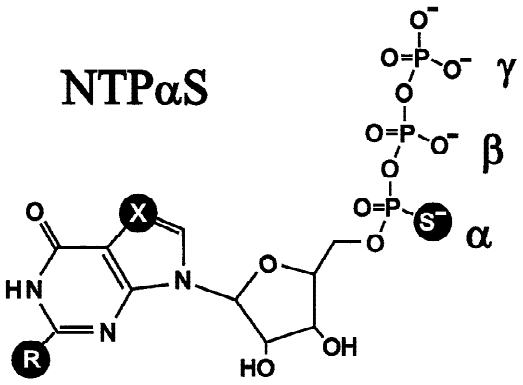

FIGURE 1. Illustration of S_p-c7-GTPαS and S_p-ITPαS analogs exploiting the phosphorothioate modification as a "reporter" for NAIM studies. Not shown is the S_p-c7-ATPαS analog also used in this study.

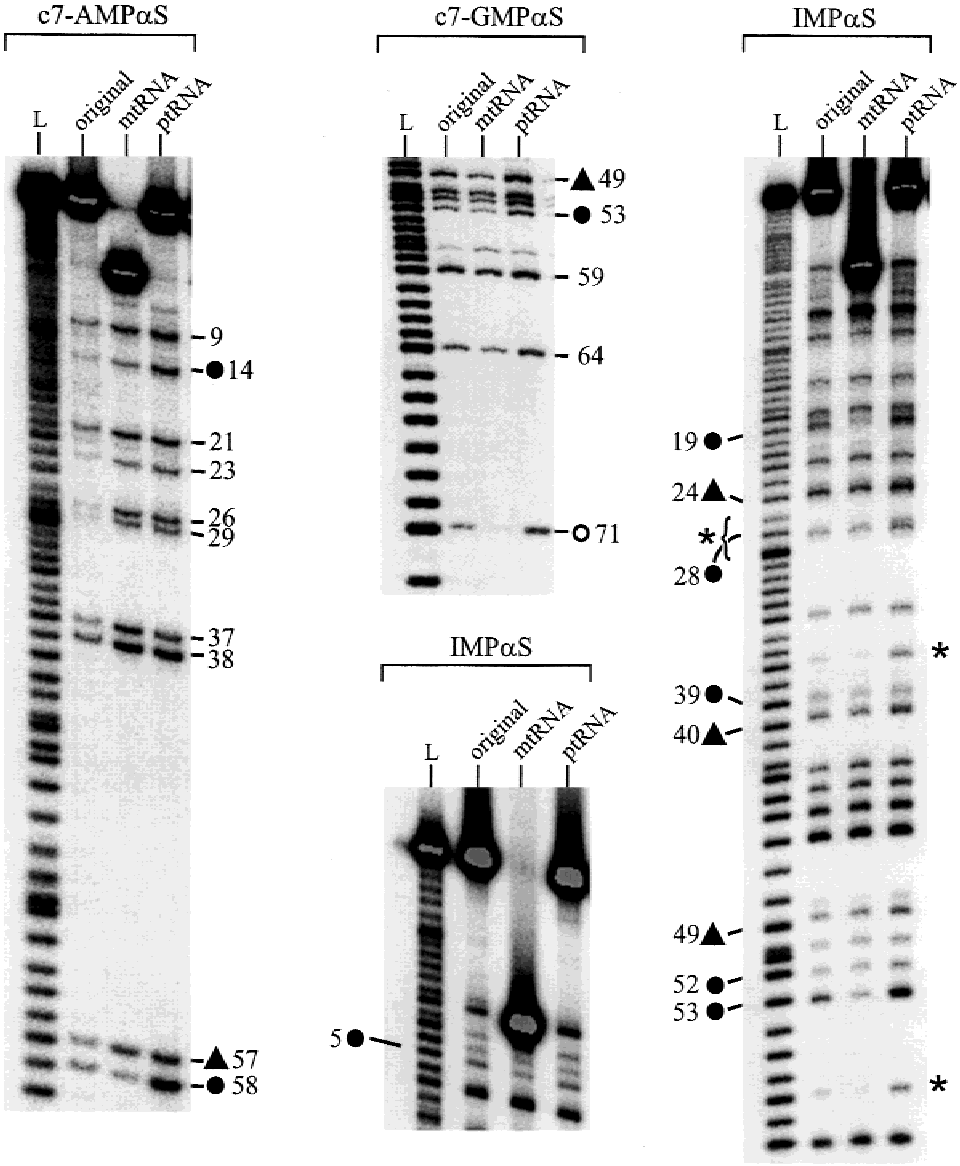

FIGURE 2. Iodine cleavage analysis of ptRNA processing interference experiments. Shown are examples of partially R_p-c7-AMPαS-, R_p-c7-GMPαS-, or R_p-IMPαS-modified pools of 3′-^{32}P-labeled ptRNA^{Gly} analyzed under conditions of 1× buffer A (see Materials and Methods). Original: the original partially modified ptRNA^{Gly} pool; mtRNA: mature tRNA^{Gly} fraction after 30–50% substrate conversion; ptRNA: unprocessed ptRNA^{Gly} fraction remaining after 30–50% substrate conversion; L: limited alkaline hydrolysis. Filled circle: nucleotide position showing c7-deaza or inosine interference; triangle: R_p-phosphorothioate-specific interference effect; open circle: combined phosphorothioate and c7-deaza interference. For further details, see Figure 3. Asterisk on the left side of the IMPαS panel: band compression in the alkaline hydrolysis ladder; asterisks on the right side of the IMPαs panel: unspecific degradation products at non-G residues and independent of iodine treatment (not shown). Note that the mtRNA lane contained less radioactive material than the ptRNA lane in the c7-GMPαS panel (see the noninterfering positions 59 and 64), which overemphasizes interference at G49, G53, and G71 at first sight.

(48%). One minor exception was a weak thioate/inosine interference effect (13%) at G18, which was only seen in the processing assay performed under tRNA binding conditions, and which was also found in the tRNA binding assay (Figs. 3B and 5). This effect may thus be specific for the high magnesium buffer system. Thioate/inosine interference effects at G24 and G40 retained the same strength when the processing assay was performed under tRNA binding conditions (17% versus 16%, and 17% versus 18%, Fig. 3A). One possible explanation is that these modifications led to an increase in the proportion of tRNA^{Gly} conformers with disruptions of contacts to RNase P RNA at multiple sites, thus becoming resistant to interference suppression under tRNA binding conditions. In comparison, interference effects at other positions, such as G5 or G52, may have been fully suppressed under tRNA binding conditions because these modifications only weakened one or a few locally confined interactions with the ribozyme.

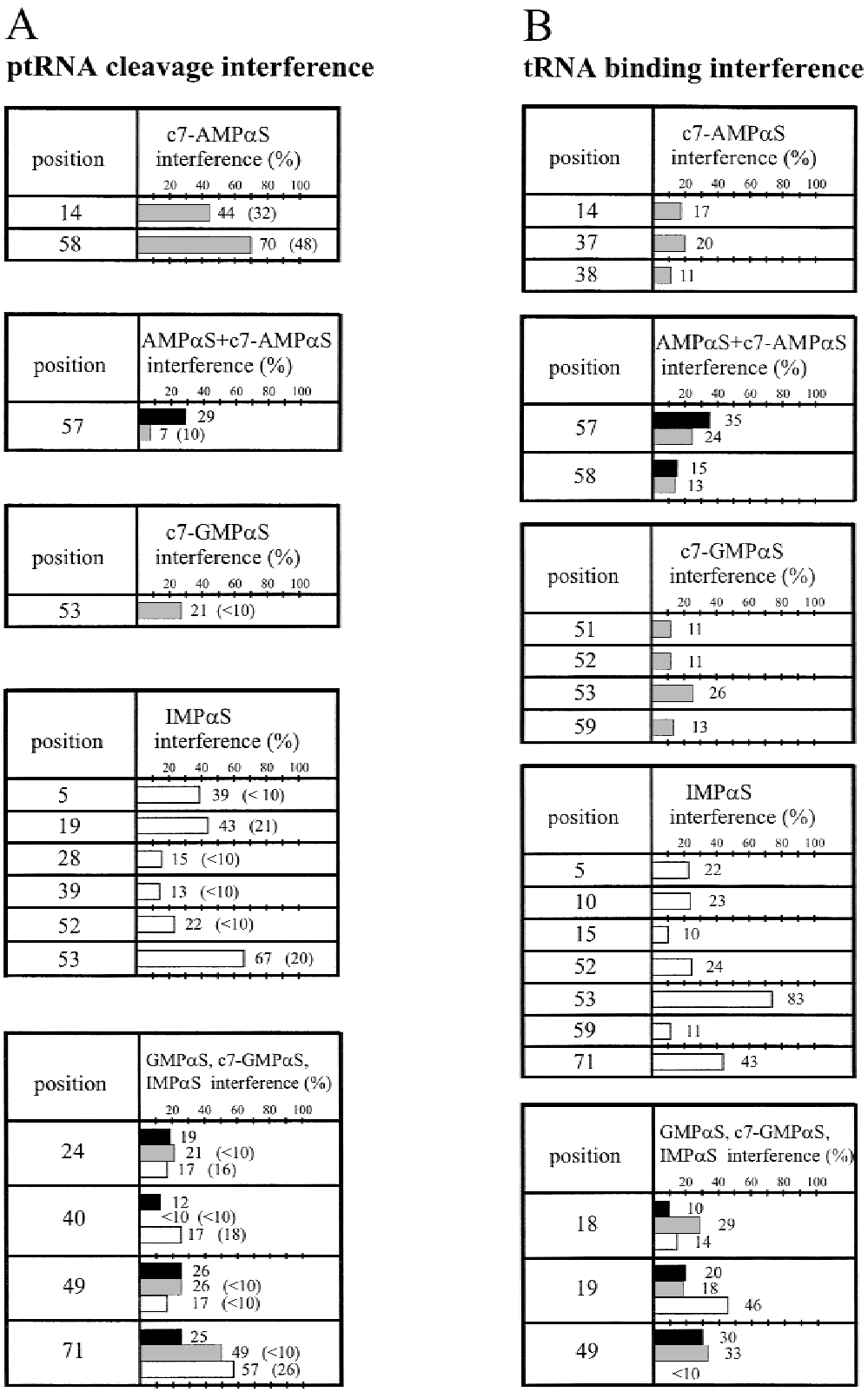

FIGURE 3. Quantification of ptRNA processing interference effects under conditions of 1× buffer A or 1× buffer B (percent values in parentheses; not tested for thioate modifications alone) (**A**); quantification of tRNA binding interference effects obtained in 1× buffer B (**B**). Data evaluation was performed with a Bio-Imaging Analyzer BAS-1000 (Fujifilm) and the software PCBAS (Raytest). Black bars: R_p-phosphorothioate interference; gray-shaded bars: c7-deaza interference; open bars: inosine interference. Each quantification was based on three to eight experiments, and deviations (averaged absolute values) between individual quantifications were below ±7%. Only sites of interference reproducibly seen and with an average percentage of ≥10 were considered significant and have been included in this figure (the value of 7% for the c7-deaza modification at A57 in **A** is shown for comparative reasons). For further details, see Materials and Methods.

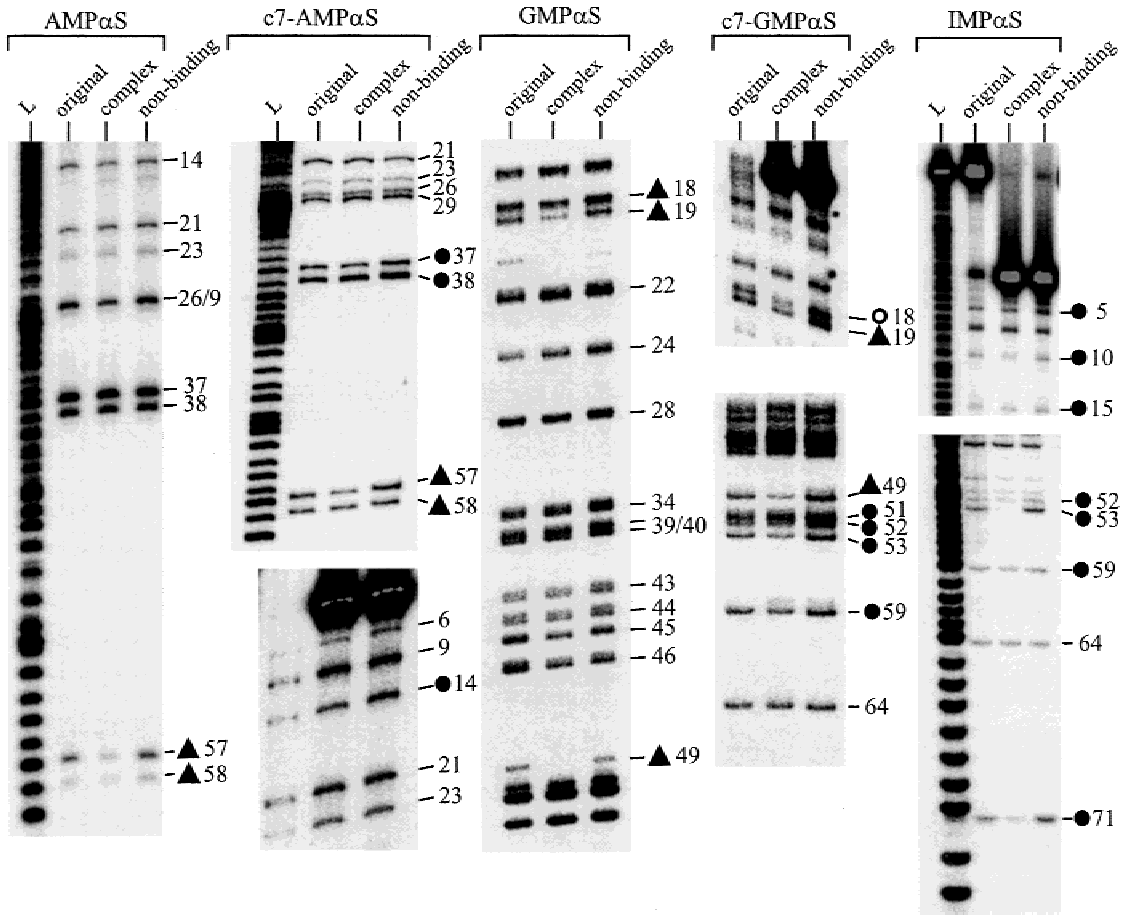

FIGURE 4. Iodine cleavage analysis of tRNA binding interference experiments. Shown are examples of partially R_p-RMPαS- (R = A, G, I) or R_p-c7-RMPαS- (R = A, G) modified pools of 3′-^{32}P-labeled tRNA^{Gly}, which were selected for *E. coli* RNase P RNA binding under conditions of 1× buffer B (see Materials and Methods). Original: the original partially modified pool; complex: tRNA^{Gly} fraction recovered from the complex with RNase P RNA; non-binding: tRNA^{Gly} fraction that did not bind to RNase P RNA; L: limited alkaline hydrolysis. Filled circle: nucleotide position showing c7-deaza or inosine interference; triangle: R_p-phosphorothioate-specific interference effect; open circle: combined phosphorothioate and c7-deaza interference. For further details, see Figure 3.

In summary, a drastic switch in the cleavage assay conditions from pH 6.0, 1 M NH_4^+, 15 mM Mg^{2+}, 0.1 μM RNase P RNA, and <1 nM of the modified substrate pool to tRNA binding conditions (pH 7.0, 0.1 M NH_4^+, 0.1 M Mg^{2+}, 0.75 μM RNase P RNA, <1 nM of the modified substrate pool, and 1 μM unmodified substrate) did basically not change the qualitative differences in the interference pattern of the processing versus the mature tRNA binding assay (Fig. 3A versus 3B). However, applying the tRNA binding conditions to the processing assay attenuated the strength of interference effects and reduced the number of significant effects to a subset of those seen under the initial processing interference conditions (Fig. 5A versus 5B).

Phosphorothioate, c7-deaza, and inosine modifications in tRNA^{Gly} that interfere with binding to RNase P RNA

Partially modified tRNAs were separated into binding and nonbinding fractions by gel retardation. Before gel loading, trace amounts (<1 nM) of the 3′-^{32}P-labeled ptRNA^{Gly} pool were incubated for 60 min at 37 °C with 0.75 μM *E. coli* RNase P RNA and excess amounts (1 μM) of unlabeled and unmodified tRNA^{Gly} in the presence of 0.1 M Mg^{2+}, 0.1 M NH_4^+ at pH 7.0 (see Materials and Methods). During this incubation step, the ptRNA pool molecules were quantitatively converted to product (see Fig. 4, upper part of the IMPαS panel). Thus, we analyzed binding of mature tRNA^{Gly}. Under the conditions applied, approximately 50% of radiolabeled pool tRNA appeared in the complex. There are two main reasons why we used radiolabeled ptRNA in the mature tRNA binding assay. First, transcription of ptRNA^{Gly}, due to its optimized 5′ terminal sequence, is more efficient than transcription of mature tRNA^{Gly}. Second, we considered it to be important to generate a pool of partially modified mature tRNA molecules with homogenous 5′-monophosphate ends because the nature of the 5′ end is expected to have an influence on mature tRNA binding to RNase P RNA. Only cleavage of ptRNA by RNase P RNA yields directly and quanti-

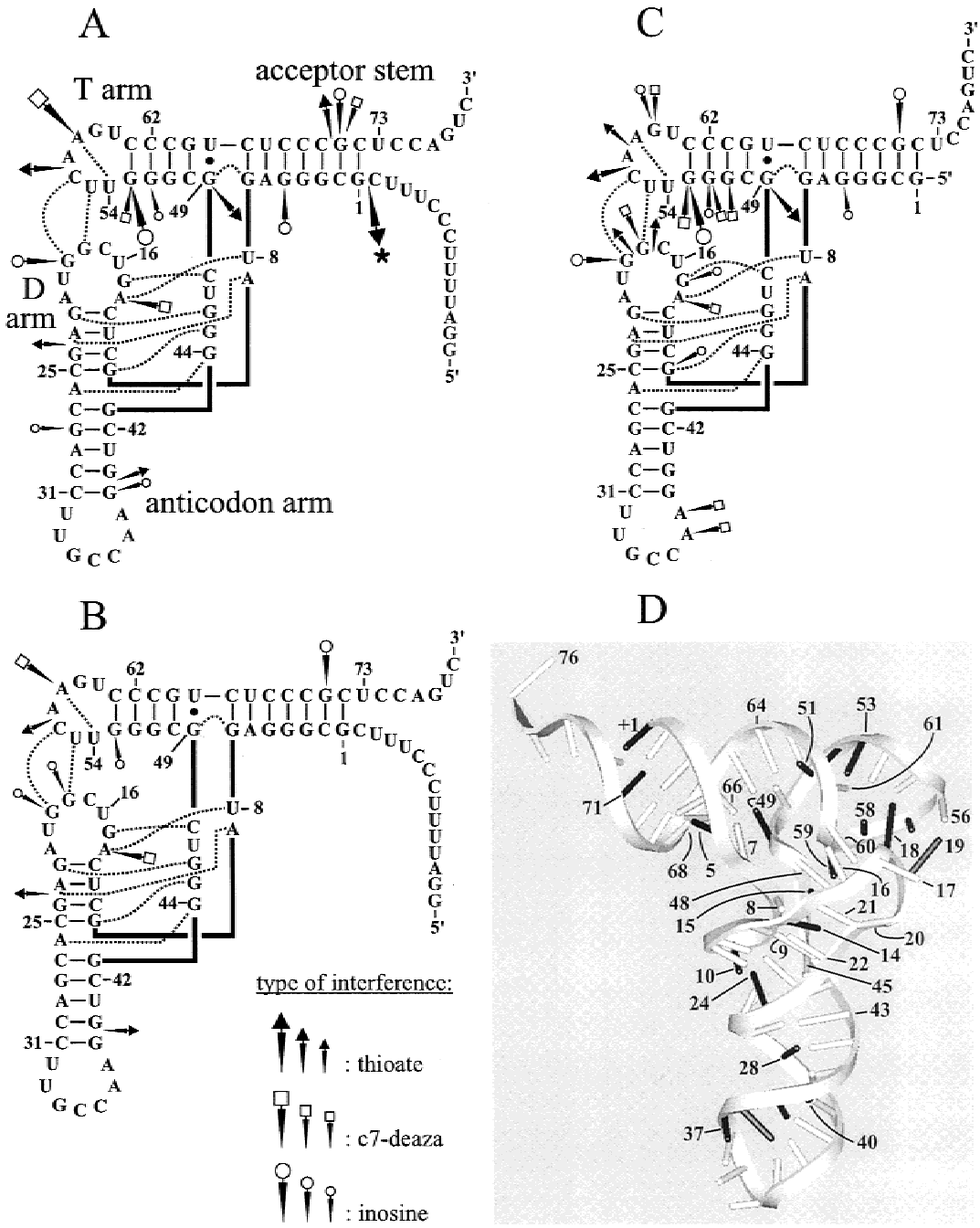

FIGURE 5. Secondary structure of *Thermus thermophilus* precursor and mature $tRNA^{Gly}$ (**A**–**C**) in the "L" arrangement according to Holbrook et al. (1978) to illustrate the relative strength of interference effects obtained in (**A**,**B**) the ptRNA processing assay under conditions of 1 × buffer A (**A**) or 1 × buffer B (**B**), or in the mature tRNA binding assay under conditions of 1 × buffer B (**C**), based on the data shown in Figure 3. Arrows with triangle: R_p-phosphorothioate interference; arrows with open square: c7-deaza interference; arrows with open circle: inosine interference. Arrow sizes indicate interference effects: >50% (large arrows), 25–50% (medium size arrows), or <25% (small arrows). Interferences <10% were not considered significant and therefore omitted. Thick lines indicate the continuity of the phosphodiester backbone. Tertiary interactions inferred from the crystal structure of yeast $tRNA^{Phe}$ (Quigley & Rich, 1976; Rich & RajBhandary, 1976; Holbrook et al., 1978) are indicated by dotted lines. Asterisk: the mode of quantification of the interference effect at G + 1 was different from that applied to all other positions (see Materials and Methods). Inosine interference at G18 in **B** may reflect a thioate interference effect as in **C**, because the GMPαS modification alone was not tested in the analysis shown in **B**. Correspondingly, interferences at G24, G40, and A57 in **B** were interpreted as thioate effects based on the results obtained under 1× buffer A conditions (**A**; see also Figure 3A). **D:** Nucleotide positions of interference (black rods) illustrated in the context of the yeast $tRNA^{Phe}$ crystal structure (Jovine et al., 2000; generated with WebLab™ ViewerLite 3.2); the nucleotide numbering system is identical to that used in **A**–**C**. The $tRNA^{Phe}$ is rotated by about 180° compared with the presentations in **A**–**C** to visualize all observed positions of interference and to better illustrate the D loop/T loop interaction at the corner of the molecule.

tatively such homogenous 5′ termini. In the case of other strategies for the synthesis of mature tRNA (initiation of transcripts with GTP, GMP, or guanosine, combined with subsequent 5′-terminal dephosphorylation/phosphorylation procedures), an undefined fraction of molecules may lack a 5′ monophosphate.

Interference effects are illustrated in Figure 4 and summarized in Figure 3B. Compared with the ptRNA^{Gly} processing NAIM analyses, identical as well as distinct interference effects were seen in the mature tRNA binding assay. C7-deaza interferences of weak (<25%) to moderate (25–50%) strength were observed at A14, A37, A38, G51, G52, G53, and G59. G18 showed a combined thioate/c7-deaza effect. Substitution of inosine for guanosine interfered at G5, G10, G15, G52, G53, G59, and G71. Inosine substitution at G53 had the most deleterious effect on tRNA^{Gly} binding to RNase P RNA (Fig. 3B). A moderate inosine interference combined with a weak thioate effect was found at G19. Interferences at G49, A57, and A58 were thioate specific. Remarkably, the c7-deaza modification at A58, which had the most deleterious effect in the processing assay, remained without effect in the tRNA binding assay (Fig. 3A versus 3B). An additional inosine interference effect seemed to be present at G4, but could not be quantified satisfactorily due to being overshadowed by excess radioactivity in the intact tRNA band (Fig. 4).

DISCUSSION

Observed interference effects do not answer the question of whether the functional group at the site of modification is involved in a direct interaction with RNase P RNA or if the modification may indirectly weaken contacts at other sites. In the first part of the following section, we will discuss interferences in the context of our current knowledge on functional groups in tRNA that directly interact with RNase P RNA. In the second part, we will discuss interferences that are likely to reflect indirect effects on substrate or product binding to RNase P RNA.

Functional tRNA groups that are candidates for direct contacts with RNase P RNA

For the following tRNA functional groups, biochemical evidence indicating their direct involvement in binding to bacterial RNase P RNA has been reported: the 2′-OH groups of residues +1, 53, 54, 56, 61, 62, 74, and possibly 57 and 72 (Perreault & Altman, 1992; Gaur & Krupp, 1993; Conrad et al., 1995; Pan et al., 1995; Loria & Pan, 1997). The 2′-OH groups of residues 54, 61, and 62 are positioned within the same minor groove due to stacking of the reversed Hoogsteen U54-A58 pair and the G53-C61 Watson–Crick pair. The binding interface involving the aforementioned 2′-OH groups may extend to the 4-amino group of C56 at the corner of the L shape (Loria & Pan, 1997). Interference effects observed in the immediate vicinity of residues 54, 56, 61, and 62, such as those at G18, G19, G53, A57, or A58 (Fig. 5), may reflect perturbations in the geometry of this binding interface. Alternatively, the phosphates at G18, G19, A57, and A58, the N7 of G18, and the 2-amine of G19 may be involved in direct contacts, as these functional groups are exposed at the tRNA corner.

Deletion of G + 1 from tRNA^{Gly} was shown to essentially abolish gel-resolvable tRNA binding (Hardt et al., 1993a), indicating the crucial role of this residue in binding to RNase P RNA. The 2′-OH of G + 1 is likely to interact directly with RNase P RNA (Perreault & Altman, 1992; Conrad et al., 1995). Moreover, there is experimental evidence that the 2-amino group of G + 1 also participates in this interaction (Kufel & Kirsebom, 1996). Methylation of N7 at G + 1 was shown to block cleavage by RNase P RNA (Kahle et al., 1990a). It has been proposed that the N7 of G + 1 may be in direct contact with RNase P RNA or may be a coordination site for a water molecule from the hydration sphere of a catalytic Mg^{2+} (Chen et al., 1997). The *pro-R_p* oxygen 5′ of G + 1 was inferred to interact with a Mg^{2+} in the transition state (Warnecke et al., 1996), explaining the strong thioate interference effect at G + 1 that rendered this position insensitive to NAIM analysis of an additional c7-deaza or inosine modification.

In the acceptor stem, we identified thioate, inosine, and c7-deaza interferences at G71, and an inosine interference at G5 (Fig. 5). This suggests that the minor groove 2-amino groups at G5 and G71 of tRNA^{Gly} as well as the *pro-R_p* oxygen and N7 of G71 can form direct contact to RNase P RNA. However, we cannot exclude the alternative possibility that a G-to-I substitution at position 71 might decrease helix stability at the end of the acceptor stem (Holbrook et al., 1978), thereby impairing tRNA recognition by RNase P RNA.

A c7-deaza interference was observed at G18 in the tRNA binding assay (Fig. 5C). The N7 of G18 is exposed at the tRNA surface and may therefore be involved in a contact with RNase P RNA. This is consistent with the finding of a cross-link between G18 and nucleotides A233 and A234 of *E. coli* RNase P RNA (Chen et al., 1998).

Modifications in tRNA^{Gly} that are likely to interfere with intramolecular tertiary interactions

The majority of interference effects in tRNA^{Gly} were identified in the acceptor stem and particularly in the D and T stem-loop regions (Fig. 5). This is consistent with previous evidence showing that the acceptor stem, CCA terminus and T arm represent major recognition elements for bacterial RNase P (reviewed in Frank & Pace, 1998). The main role of the D stem-loop is most likely to organize the T loop structure and to support the

angle (14° in $tRNA^{Phe}$; Holbrook et al., 1978) between the two helical axes of the acceptor stem and the T stem (Hardt et al., 1993b). Several of the observed interference effects (Fig. 5) reflect the perturbation of known intramolecular tertiary interactions identified in crystal structures of yeast $tRNA^{Phe}$ (Rich & RajBhandary, 1976), which, like $tRNA^{Gly}$, represents a typical class I tRNA with a 4-bp D stem and a 5-nt variable loop. Involvement of N7 of the conserved A14 in a reversed Hoogsteen base pair with U8 explains the c7-deaza interference at A14. The same pertains to the A58-U54 reversed Hoogsteen base pair (Fig. 5A,B).

The weak R_p-phosphorothioate effect at A58 (Fig. 5C) may be explained by hydrogen bonding between the phosphate of A58 and N3 of U55. This contact was proposed to stabilize the sharp turn of the T loop (Rich & RajBhandary, 1976). The *pro-R_p* oxygen (O2P) of nt 57 is also in hydrogen bonding distance to the N3 of pseudouridine 55 in yeast $tRNA^{Phe}$ (Jovine et al., 2000), and, by inference, to the N3 of U55 in $tRNA^{Gly}$, which could account for the thioate interference effect at A57 (Fig. 3). The conserved G19-C56 pair, the only tertiary Watson–Crick base pair in the yeast $tRNA^{Phe}$ crystal structure, has a central role in connecting the D to the T loop (Fig. 5D). This base pair was reported to be strained and less stable than a normal G-C pair due to being twisted and also bent by about 30° from planarity (Holbrook et al., 1978). This may explain the impairment of function due to elimination of one hydrogen bond by inosine substitution for G19 (Fig. 5). Strong inosine interference was seen at G53 in both assays. The conservation of the G53-C61 base pair is explained by a T loop-stabilizing contact between N4 of C61 and the *pro-S_p* oxygen (O1P) of nucleotide 60. The G53-C61 pair is also expected to stack on the U54-A58 reversed Hoogsteen pair (Rich & RajBhandary, 1976) and on the G52-C62 base pair. Destabilization of the T loop structure due to a weakening of the G53-C61 pair could explain the inosine interference effect at position 53 (Fig. 5). The c7-deaza interference at G53 may be due to impaired stacking of G53 with G52 and/or U54. The clustering of interference effects in the D and T loop may also be related to a destabilization of the base-stacking interactions occurring in the sequence G19-A57-G18-A58, in analogy to the situation in yeast $tRNA^{Phe}$ (Holbrook et al., 1978). Based on the present three-dimensional models (Chen et al., 1998; Massire et al., 1998), inosine and c7-deaza interferences at G51 to G53 might also indicate that 2-NH_2 and/or N7 functions at these positions form direct contacts with RNase P RNA.

Destabilization of the G15-C48 reversed Watson–Crick base pair in the tRNA core may account for the weak inosine interference seen at G15 in the tRNA binding assay. A hydrogen bond between the 2′-OH of U7 and the phosphate of m^5C49 in yeast $tRNA^{Phe}$ is thought to stabilize the coaxial stack of acceptor and T stem (Quigley & Rich, 1976; Jovine et al., 2000). This could explain the thioate interference at G49 (Fig. 5A,C), assuming a similar scenario for $tRNA^{Gly}$ despite the different base identities at these positions (G7, G49). Thioate interference at G19 is accounted for by disruption of a hydrogen bond formed between the 2′-OH of C17 and the *pro-R_p* oxygen (O2P) of G19 (Quigley & Rich, 1976; Jovine et al., 2000). Also, some of the D and T stem-loop interferences may have resulted from perturbation of a strong Mg^{2+} binding site that bridges and thereby stabilizes the D and T loop region in yeast $tRNA^{Phe}$ (Jack et al., 1977). In yeast $tRNA^{Phe}$, this Mg^{2+} is in direct bonding distance to G19-O1P, and can be linked through water molecules to U59-O4, C60-N3, G20-O6, and G20-N7 (Jack et al., 1977). Because $tRNA^{Gly}$ has a G at position 59, and U residues at positions 20 and 60, binding of a Mg^{2+} in this area of $tRNA^{Gly}$ would involve other coordination sites and is therefore speculative at present.

Interference effects in the D stem and anticodon arm

Surprisingly, weak to moderate interferences were identified at G10, G24, G28, A37, A38, G39, and G40 (Fig. 5). These residues are part of the long vertical stack protruding from the tRNA core region (Rich & RajBhandary, 1976; Fig. 5D). Because these residues are remote from the assumed tRNA–RNase P RNA binding interface, they probably represent indirect effects, either by favoring aberrant tRNA folding and/or by transmitting changes in local conformation to the corner of the L shape. In fact, it has been proposed for the crystal structure of yeast $tRNA^{Asp}$ that conformational changes in the anticodon loop (e.g., those caused by anticodon–anticodon pairing between adjacent molecules in the crystal) are propagated through the anticodon arm to the D loop, resulting in destabilization and increased flexibility of the D and T loop region (Westhof et al., 1985). Also, G37 of yeast $tRNA^{Phe}$ (corresponding to the Y base in modified $tRNA^{Phe}$) was one of a few residues with increased local disorder or large-scale mobility in the crystal structure (Westhof & Sundaralingam, 1986). Assuming a similar situation for $tRNA^{Gly}$, A37/38 might represent a nucleation point for conformational changes in this anticodon loop as well. C7-deaza modifications at A37/38 may favor such a conformational switch resulting in a flexibility transfer to the D loop.

Synopsis

In Table 1, observed interference effects have been classified according to their probability to reflect the perturbation of direct intermolecular contacts to RNase P RNA, based on the knowledge that acceptor arm and T arm provide the main contact surface for bacterial

TABLE 1. Modifications in tRNA moieties interfering with binding to and/or processing by bacterial RNase P RNA: classification according to the probability that interferences reflect the perturbation of direct intermolecular contacts to RNase P RNAs rather than indirect effects, such as the disruption of intramolecular tertiary contacts in tRNA. Compare with tRNA architecture shown in Figure 5D.

Type of modification/ interference positions/ tRNA species	Study	Direct contact	Comments[a]
Thioate modification:			
G19, G24, G40, G49, tRNA(Gly)	Figure 3	no	—remote from binding interface, H-bond G19 O2P-N17 O2′ (8)
G18, A57, A58, tRNA(Gly)	Figure 3	?	—solvent-exposed at tRNA corner
G + 1, G71, tRNA(Gly)	Figures 3, 5A	?	
U9, tRNA(Tyr)	(1, 2)	no	—remote from binding interface
G2, tRNA(Tyr)	(2)	yes	
A9, tRNA(Phe)	(1, 2)	no	—remote from binding interface
C2, U54/55, tRNA(Phe)	(1, 2)	yes	—no gel resolution of U54/55
U68/69, tRNA(Phe)	(1, 2)	?	—no gel resolution of U68/69
Inosine modification:			
G5, G19, G52, G53, G71, tRNA(Gly)	Figure 3	?	
G10, G15, G28, G39, G59, tRNA(Gly)	Figure 3	no	
c7-deaza modification:			
G + 1, tRNA(Su3)	(3)	yes	—remote from binding interface (G10, G28, G39), organization of core structure (G15, G59)
A14, A37, A38, A58, G59, tRNA(Gly)	Figure 3	no	—N59 projecting from the T loop, stacks on G15-C48 pair (8, 9)
G18, tRNA(Gly)	Figure 3	yes	
G51, G52, G53, G71, tRNA(Gly)	Figure 3	?	
N7-methyl-G:			
G + 1, tRNA(Ser)	(4)	?	
2′-deoxy modification:			
U54, C56, C61, A62, C74, tRNA(Phe)	(5, 6)	yes	—*B. subtilis* RNase P RNA
G57, C72, tRNA(Phe)	(6)	?	—*B. subtilis* RNase P RNA
U54, tRNA(Tyr)	(1)	yes	—using R_p-dTMPαS, no gel resolution of U54/55, H-bond G57 N7–N55 O2′ (8)
U55, tRNA(Tyr)	(1)	no	
G + 1, G53 tRNA(Phe)	(2)	yes	
G3, G57, tRNA(Phe)	(2)	?	
A58, tRNA(Phe)	(1, 2)	no	—H-bond A58 O2′–C60 O2P (8)
G + 1, C74	(7)	yes	—hairpin model substrate
C2, C72, A73	(7)	?	—hairpin model substrate

[a]Unless otherwise stated, interference effects were observed with *E. coli* RNase P RNA. (1) Gaur & Krupp, 1993; (2) Conrad et al., 1995; (3) Kufel & Kirsebom, 1996; (4) Kahle et al., 1990a; (5) Loria & Pan, 1997; (6) Pan et al., 1995; (7) Perreault & Altman, 1992; (8) Quigley & Rich, 1976; (9) Rich & RajBhandary, 1976.

RNase P RNA. Other modifications have been interpreted to affect binding to RNase P RNA by indirect means, either by disrupting known intramolecular tertiary contacts in tRNA and/or changing the conformational equilibrium of $tRNA^{Gly}$. Question marks in Table 1 indicate interference effects for which we considered the interpretation to be too speculative at present. This includes several interferences observed at positions in the acceptor stem, such as G5 and G71, which are candidates for direct contacts but are more than 10 Å away from any functional group of RNase P RNA in the current (static) three-dimensional models (Chen et al., 1998; Massire et al., 1998). For comparison, functional groups in tRNA identified to be important for interaction with bacterial RNase P RNA in previous studies have been included in Table 1.

Differential interference pattern obtained in the tRNA binding and ptRNA processing assays

Although many of the observed interferences are likely to represent indirect effects, they nevertheless provide useful information to assess differences in the binding mode of precursor versus mature tRNA. The overlapping but distinct interference patterns observed in the processing and mature tRNA binding assays of this study indeed indicate such differences. The following effects were observed both in the ptRNA processing and tRNA binding assays: thioate interference at G49 and A57; inosine interference at G5, G19, G52, G53, and G71; and c7-deaza interferences at A14 and G53. Unique to the processing assay were weak thio-

ate interferences at G24, G40, and G71, inosine interferences at G28 and G39, and c7-deaza interferences at A58 and G71. Effects exclusively found in the tRNA binding assay included thioate interferences at G18, G19, and A58, inosine interferences at G10, G15, and G59, as well as several weak c7-deaza interferences (G18, A37, A38, G51, G52, and G59)

The processing assays were performed under two largely different conditions. In the first setup (1 M NH_4^+, 15 mM Mg^{2+}, pH 6.0, ribozyme concentration below the single turnover K_m), it is likely that the lower Mg^{2+} concentration rendered ptRNA-RNase P RNA complex formation relatively sensitive to structural perturbations. NAIM analyses with the catalytic RNA moiety have established that increasing Mg^{2+} concentrations can suppress interference effects (Kazantsev & Pace, 1998). In addition, at the low pH of 6.0, the chemical step is slower than at pH 7.0 (Smith & Pace, 1993), which means that the ratio of k_{chem} (the rate for the chemical step) to k_{-1} (the off-rate for the substrate) decreases. As a consequence, more ptRNAs with minor structural perturbations will dissociate from the ribozyme before cleavage occurs.

In the second setup, we performed the ptRNA processing NAIM analysis in the presence of exactly the same RNA concentrations and under identical buffer conditions (0.1 M NH_4^+, 0.1 M Mg^{2+}, pH 7.0) as used for the tRNA binding assay. Due to the higher Mg^{2+} concentration and/or the faster chemical step (and possibly the higher ribozyme concentration), several interference effects disappeared (Fig. 5A versus 5B). However, with the single exception of a minor interference at G18, no new interference effects appeared under these conditions compared with the low Mg^{2+}/pH 6.0 processing conditions. Thus, the distinct differences in the interference pattern obtained with the tRNA binding versus the ptRNA processing assay persisted. From these results we conclude that substrate binding and cleavage involves binding modes or conformational states distinct from the binding mode of mature tRNA, the product of the reaction.

Correlation of binding interference data obtained on the $tRNA^{Gly}$ and *E. coli* RNase P RNA level

Based on the crystal structure of yeast $tRNA^{Phe}$, a class I tRNA very similar to the $tRNA^{Gly}$ used here, we were able to interpret a significant proportion of inosine and c7-deaza interference effects in terms of disruption of crucial intramolecular tertiary contacts within tRNA. The strongest effects obtained in the processing and/or tRNA binding assays were at conserved nucleotide positions (A14, G19, G53, A58). Extrapolating our findings obtained on the tRNA level to corresponding interference patterns obtained for RNase P RNA itself, whose complex three-dimensional structure is expected to depend on even more extensive networks of tertiary interactions than that of tRNA molecules (see below), we infer that many if not the majority of inosine and c7-deaza modifications found to impair RNase P RNA function (Heide et al., 1999; unpubl. results) are likely to represent perturbations of RNase P RNA tertiary structure rather than reflecting functional groups involved in direct contacts with the tRNA moiety.

R_p-phosphorothioate, inosine, and c7-deaza modifications of purines that destabilize gel-resolvable binding of $tRNA^{Gly}$ to *E. coli* RNase P RNA have been determined for both RNA molecules under very similar conditions (Hardt et al., 1995b; Heide et al., 1999; this study; our unpubl. results). We identified only one strong (>50%) binding interference effect in $tRNA^{Gly}$ (at G53, Fig. 3B). However, for RNase P RNA that is five times the length of tRNA, we identified, apart from interference effects at G292 and G293 representing direct tRNA–ribozyme contacts (Kirsebom & Svärd, 1994; Heide et al., 1999; Busch et al., 2000), a total of more than 20 strong binding interference effects, attributable to a single thioate, inosine, or c7-deaza modification at one of the purine positions (Heide et al., 1999; our unpubl. results). This comparison allows us to gain an impression of how many more crucial tertiary interactions seem to be required to maintain the complex structure of a ribozyme the size of RNase P RNA.

CONCLUSIONS

We have identified R_p-phosphorothioate, c7-deaza, and inosine modifications in a bacterial $tRNA^{Gly}$ that interfere with processing by *E. coli* RNase P RNA or reduce the binding affinity of mature tRNA, the product of the reaction. The strongest interference effects were observed at positions G19, G53, A58, and G71 located in the D arm, T arm, and acceptor stem, which are known to provide the main recognition elements for RNase P. Only a minor fraction of affected functional groups (at G5, G18, and G71) are candidates for direct contacts with RNase P RNA. Many interferences could be interpreted as disrupting intramolecular tertiary contacts known to stabilize the authentic tRNA fold. Interference patterns obtained in the substrate processing and mature tRNA binding assays were overlapping but distinct. A change in the processing assay conditions to those of the mature tRNA binding assay, leading to faster substrate conversion, reduced or suppressed most interference effects, but did not reveal new sites of interference except for the appearance of a weak inosine/thioate effect at G18. Thioate interference at G49 and A57, inosine interferences at G5, G19, G52, G53, and G71, and c7-deaza interferences at A14 and G53 were seen in both assays. The largest discrepancy was the c7-deaza interference effect at A58, which represented the strongest interference effect in the processing assays, but was not detectable in the mature

tRNA binding assay. Thus, our results indicate that substrate binding and cleavage involve binding modes or conformational states distinct from the binding mode of mature tRNA, the product of the reaction. It will be intriguing to include the protein component of RNase P in future NAIM analyses to investigate its influence on substrate and product binding modes.

MATERIALS AND METHODS

Preparation of RNAs

Mature tRNA^{Gly}CCAAUA (used as competitor in gel retardation experiments; see below) was synthesized by runoff transcription with T7 RNA polymerase from a PCR template (Heide et al., 1999), *E. coli* RNase P RNA and ptRNA^{Gly}CCAGUC (Fig. 5) from plasmids pSP64M1HH (Heide et al., 1999) and pSBpt3′hh, respectively, linearized with *Bam*HI and encoding *cis*-cleaving hammerhead structures to generate homogeneous 3′ ends; tRNA^{Gly}CCAAUA and tRNA^{Gly}CCAGUC bind with identical affinity to *E. coli* RNase P RNA (Busch et al., 2000). Unmodified *E. coli* RNase P RNA and mature and precursor tRNA^{Gly} were transcribed and purified exactly as described (Heide et al., 1999). For the synthesis of phosphorothioate-modified ptRNA^{Gly}, purines were partially replaced with the S_p-NTPαS, S_p-c7-RTPαS (Kazantsev & Pace, 1998), or S_p-ITPαS (NAPS Göttingen, Germany) analog. Partially modified ptRNA pools were transcribed with T7 RNA polymerase under the following conditions (40 μL assay): 80 mM HEPES/HCl, pH 7.5, 22 mM $MgCl_2$, 1 mM spermidine, 4.8 μg BSA, 5 mM DTT, 1 U pyrophosphatase (Roche Molecular Biochemicals), 2 μg linearized plasmid DNA, 200–400 U T7 RNA polymerase (MBI Fermentas), and the following NTP and analog concentrations: for R_p-A(G)MPαS and R_p-c7-RMPαS modifications, for example, of A residues, 0.9 mM ATP, 1 mM each CTP, GTP, and UTP, and 0.1 mM S_p-ATPαS or S_p-c7-ATPαS; for R_p-IMPαS modifications, transcription was performed in the presence of 40 mM Tris-HCl, pH 8.0, 2 mM NaCl, 8 mM $MgCl_2$, 2 mM spermidine, 5 mM DTT, 1 mM GTP, 1.5 mM each ATP, CTP, and UTP, 0.1 mM S_p-ITPαS, 2 μg linearized plasmid DNA and 200–400 U T7 RNA polymerase. After digestion with DNase I, transcription assays were purified as described (Heide et al., 1999).

End labeling

5′- and 3′-end labeling and removal of 2′,3′ cyclic phosphates after hammerhead self-cleavage was performed as described (Heide et al., 1999).

Cleavage interference

Single turnover experiments were performed with trace amounts of phosphorothioate-modified 3′-^{32}P-labeled ptRNA^{Gly} pools and 0.1 μM *E. coli* RNase P RNA in 1× buffer A [50 mM MES, pH 6.0 at 37 °C, 1 M NH_4OAc, and 15 mM $Mg(OAc)_2$]. RNase P RNA (0.2 μM) was preincubated separately for 1 h at 37 °C and the ptRNA pool for 5 min at 55 °C and for 25 min at 37 °C under cleavage assay conditions before starting the reaction by combining equal volumes of prewarmed enzyme and substrate mixtures. The processing reaction was stopped after approximately 3 min by the addition of 400 μL H_2O, when 30–50% of the substrate had been converted to product. The reaction mixture was precipitated with ethanol in the presence of 75 mM NaOAc, pH 6.7, dissolved in 20 μL loading buffer (67% formamide, 30 mM boric acid, 30 mM Tris-HCl, pH 8.3, 0.7 mM EDTA, 2.7 M urea, 0.01% [w/v] each BPB and XCB) and analyzed by 8% PAGE in the presence of 8 M urea. The bands corresponding to mature and precursor tRNA were excised from gels, eluted, precipitated by ethanol, and subjected to iodine hydrolysis (Heide et al., 1999). To analyze cleavage interference under tRNA binding conditions, single turnover experiments were performed as follows: 1.5 μM RNase P RNA was preincubated for 60 min at 37 °C in 1× buffer B (see below); 2 μM unlabeled competitor ptRNA^{Gly} and trace amounts of the partially modified 3′-^{32}P-labeled ptRNA^{Gly} pool were preincubated for 5 min at 55 °C and for 25 min at 37 °C in 1× buffer B. Reactions were started by combining equal volumes of enzyme and substrate mixtures to give final concentrations of 0.75 μM RNase P RNA and 1 μM unlabeled competitor ptRNA^{Gly}. Samples were further treated as described above, except that reactions were stopped after approximately 50 s due to the higher turnover rate under these conditions.

Gel retardation

Gel retardation was essentially performed as described previously (Hardt et al., 1995a). To analyze binding of partially phosphorothioate-modified tRNA^{Gly} pools to *E. coli* RNase P RNA, 1.5 μM RNase P RNA and 2 μM unlabeled competitor tRNA^{Gly} were preincubated for 60 min at 37 °C in 1× buffer B [100 mM $Mg(OAc)_2$, 100 mM NH_4OAc, 1 mM EDTA, 50 mM TrisOAc, pH 7.0 at 37 °C] containing 10% glycerol; trace amounts of the 3′-^{32}P-labeled ptRNA^{Gly} pool were preincubated separately for 5 min at 55 °C and 25 min at 37 °C in 1× buffer B. Equal volumes of the two RNA solutions were combined to give final concentrations of 0.75 μM RNase P RNA, 1 μM unlabeled competitor tRNA^{Gly}, and 5% glycerol in 1× buffer B, followed by incubation for 60 min at 37 °C, resulting in essentially complete maturation of the 3′-^{32}P-labeled ptRNA^{Gly} pool. Samples were loaded on a native 7.5% polyacrylamide gel and run for 3–4 h at 37 °C. Bands corresponding to bound and unbound tRNA were visualized by autoradiography, excised from the gel, and polymerized into a 7% PAA/8 M urea gel followed by electrophoresis under 1× TBE conditions. After autoradiography, tRNA bands were excised again, eluted, and concentrated as described (Heide et al., 1999).

Iodine hydrolysis

Iodine hydrolysis and quantification of interference effects was performed as described previously (Heide et al., 1999). Hydrolysis bands were analyzed on 6%, 8%, 10%, 15%, or 25% PAA/8 M urea gels, and visualized and quantified using a Bio-Imaging Analyzer BAS-1000 (Fujifilm) and the analysis software PCBAS (Raytest). In the case of the tRNA binding assay, interference effects for individual bands were quantified as follows: $f_{\text{non-bind.}} = [I_{\text{non-bind.}}/(I_{\text{non-bind.}} + I_{\text{complex}})] \times 100\%$ and $f_{\text{complex}} = [I_{\text{complex}}/(I_{\text{non-bind.}} + I_{\text{complex}})] \times 100\%$, with $f_{\text{non-bind.}}$ and f_{complex} indicating the fractional intensities of the non-binding and binding (complex) tRNA fractions, respectively.

Intensities (I) were corrected for background values and were normalized to the average intensities of three or more reference bands for which an interference effect was not apparent. For example, if the aforementioned three or more reference bands showed an average reduction in intensity by a factor of 0.8 in the lane corresponding to the RNase P RNA fraction from the complex, $I_{complex}$ was divided by this factor to avoid overemphasizing the interference effect. Finally, interference effects (in percent, Fig. 3) were determined by subtracting the corrected $f_{complex}$ value from the $f_{non\text{-}bind.}$ value. In the case of the processing assay, the data evaluation was identical, except that $f_{uncleaved}$ and $f_{cleaved}$ instead of $f_{non\text{-}bind.}$ and $f_{complex}$ were calculated. For processing interference at G + 1, the normalized intensity of the corresponding band in the unreacted ptRNA fraction was divided by the normalized intensity of the G + 1 band in the original ptRNA pool.

ACKNOWLEDGMENTS

We are grateful to Alexei V. Kazantsev and Norman R. Pace for the gift of S_p-c7-ATPαS and S_p-c7-GTPαS, and Tina Persson for critical reading of the manuscript.

Received August 31, 2000; returned for revision September 29, 2000; revised manuscript received January 5, 2001

REFERENCES

Altman S, Kirsebom LA. 1999. Ribonuclease P. In: Gesteland RF, Cech T, Atkins JF, eds. *The RNA world*. Cold Spring Harbor, New York: Cold Spring Harbor Laboratory Press. pp 351–380.

Busch S, Kirsebom LA, Notbohm H, Hartmann RK. 2000. Differential role of the intermolecular base pairs G292-C_{75} and G293-C_{74} in the reaction catalyzed by *Escherichia coli* RNase P RNA. *J Mol Biol 299*:941–951.

Chen J-L, Nolan JM, Harris ME, Pace NR. 1998. Comparative photocrosslinking analysis of the tertiary structure of *Escherichia coli* and *Bacillus subtilis* RNase P RNAs. *EMBO J 17*:1515–1525.

Chen Y, Li X, Gegenheimer P. 1997. Ribonuclease P catalysis requires Mg^{2+} coordinated to the *pro-R_p* oxygen of the scissile bond. *Biochemistry 36*:2425–2438.

Christian EL, Yarus M. 1992. Analysis of the role of phosphate oxygens in the group I intron from *Tetrahymena*. *J Mol Biol 228*:743–758.

Conrad F, Hanne A, Gaur RK, Krupp G. 1995. Enzymatic synthesis of 2′-modified nucleic acids: Identification of important phosphate and ribose moieties in RNase P substrates. *Nucleic Acids Res 23*:1845–1853.

Frank DN, Pace NR. 1998. Ribonuclease P: Unity and diversity in a tRNA processing ribozyme. *Ann Rev Biochem 67*:153–180.

Gaur RK, Hanne A, Conrad F, Kahle D, Krupp G. 1996. Differences in the interaction of *Escherichia coli* RNase P RNA with tRNAs containing a short or a long extra arm. *RNA 2*:674–681.

Gaur RK, Krupp G. 1993. Modification interference approach to detect ribose moieties important for the optimal activity of a ribozyme. *Nucleic Acid Res 21*:21–26.

Guerrier-Takada C, Altman S. 1993. A physical assay for and kinetic analysis of the interactions between M1 RNA and tRNA precursor substrates. *Biochemistry 32*:7152–7161.

Guerrier-Takada C, Gardiner K, Marsh T, Pace N, Altman S. 1983. The RNA moiety of ribonuclease P is the catalytic subunit of the enzyme. *Cell 35*:849–857.

Hardt WD, Schlegl J, Erdmann VA, Hartmann RK. 1993a. Gel retardation analysis of *E. coli* M1 RNA–tRNA complexes. *Nucleic Acids Res 21*:3521–3527.

Hardt W-D, Schlegl J, Erdmann VA, Hartmann RK. 1993b. Role of the D arm and the anticodon arm in tRNA recognition by eubacterial and eukaryotic RNase P enzymes. *Biochemistry 32*:13046–13053.

Hardt WD, Schlegl J, Erdmann VA, Hartmann RK. 1995a. Kinetics and thermodynamics of the RNase P RNA cleavage reaction: Analysis of tRNA 3′-end variants. *J Mol Biol 247*:161–172.

Hardt W-D, Warnecke JM, Erdmann VA, Hartmann RK. 1995b. R_p-phosphorothioate modifications in RNase P RNA that interfere with tRNA binding. *EMBO J 14*:2935–2944.

Heide C, Pfeiffer T, Nolan JM, Hartmann RK. 1999. Guanosin 2-NH_2 groups of *Escherichia coli* RNase P RNA involved in intramolecular tertiary contacts and direct interactions with tRNA. *RNA 5*:102–116.

Holbrook SR, Sussmann JL, Warrant RW, Kim SH. 1978. Crystal structure of yeast phenylalanine transfer RNA. *J Mol Biol 123*:631–660.

Jack A, Ladner JE, Rhodes D, Brown RS, Klug A. 1977. A crystallographic study of metal-binding to yeast phenylalanine transfer RNA. *J Mol Biol 111*:315–328.

Jovine L, Djordjevic S, Rhodes D. 2000. The crystal structure of yeast phenylalanine tRNA at 2.0 Å resolution: Cleavage by Mg^{2+} in 15-year old crystals. *J Mol Biol 301*:401–414.

Kahle D, Wehmeyer U, Char S, Krupp G. 1990a. The methylation of one specific guanosine in a pre-tRNA prevents cleavage by RNase P and by the catalytic M1 RNA. *Nucleic Acids Res 18*:837–844.

Kahle D, Wehmeyer U, Krupp G. 1990b. Substrate recognition by RNase P and by the catalytic M1 RNA: Identification of possible contact points in pre-tRNAs. *EMBO J 9*:1929–1937.

Kazantsev AV, Pace NR. 1998. Identification by modification-interference of purine N-7 and ribose 2′-OH groups critical for catalysis by bacterial ribonuclease P. *RNA 4*:937–947.

Kirsebom LA, Svärd SG. 1994. Base pairing between *Escherichia coli* RNase P RNA and its substrate. *EMBO J 13*:4870–4876.

Kufel J, Kirsebom LA. 1996. Different cleavage sites are aligned differently in the active site of M1 RNA, the catalytic subunit of *Escherichia coli* RNase P. *Proc Natl Acad Sci USA 93*:6085–6090.

Loria A, Pan T. 1997. Recognition of the T stem-loop of a pre-tRNA substrate by the ribozyme from *Bacillus subtilis* ribonuclease P. *Biochemistry 36*:6317–6325.

Massire C, Jaeger L, Westhof E. 1998. Derivation of the three-dimensional architecture of bacterial ribonuclease P RNAs from comparative sequence analysis. *J Mol Biol 279*:773–793.

Oh BK, Frank DN, Pace NR. 1998. Participation of the 3′-CCA of tRNA in the binding of catalytic Mg^{2+} ions by ribonuclease P. *Biochemistry 37*:7277–7283.

Oh BK, Pace NR. 1994. Interaction of the 3′-end of tRNA with ribonuclease P RNA. *Nucleic Acids Res 22*:4087–4094.

Pan T, Loria A, Zhong K. 1995. Probing of tertiary interactions in RNA: 2′-hydroxyl-base contacts between the RNase P RNA and pre-tRNA. *Proc Natl Acad Sci USA 92*:12510–12514.

Pannucci JA, Haas ES, Hall TA, Harris JK, Brown JW. 1999. RNase P RNAs from some Archaea are catalytically active. *Proc Natl Acad Sci USA 96*:7803–7808.

Perreault J-P, Altman S. 1992. Important 2′-hydroxyl groups in model substrates for M1 RNA, the catalytic RNA subunit of RNase P from *Escherichia coli*. *J Mol Biol 226*:399–409.

Pomeranz Krummel DA, Altman, S. 1999. Multiple binding modes of substrate to the catalytic RNA subunit of RNase P from *Escherichia coli*. *RNA 5*:1021–1033.

Quigley GJ, Rich A. 1976. Structural domains of transfer RNA molecules. *Science 194*:796–806.

Rich A, RajBhandary UL. 1976. Transfer RNA: Molecular structure, sequence, and properties. *Annu Rev Biochem 45*:805–860.

Smith D, Pace NR. 1993. Multiple magnesium ions in the ribonuclease P reaction mechanism. *Biochemistry 32*:5273–5281.

Warnecke JM, Fürste JP, Hardt WD, Erdmann VA, Hartmann RK. 1996. Ribonuclease P is converted to a Cd^{2+}-ribozyme by a single R_p-phosphorothioate modification in the precursor tRNA at the RNase P cleavage site. *Proc Natl Acad Sci USA 96*:8924–8928.

Westhof E, Dumas P, Moras D. 1985. Crystallographic refinement of yeast aspartic acid transfer RNA. *J Mol Biol 184*:119–145.

Westhof E, Sundaralingam M. 1986. Restrained refinement of the monoclinic form of yeast phenylalanine transfer RNA. Temperature factors and dynamics, coordinated waters, and base-pair propeller twist angles. *Biochemistry 25*:4868–4878.

Westhof E, Wesolowski D, Altman S. 1996. Mapping in three dimensions of regions in a catalytic RNA protected from attack by an Fe(II)-EDTA reagent. *J Mol Biol 258*:600–613.